DECREASED EXPRESSION OF MITOCHONDRIAL ATP SYNTHASE SUBUNIT D (A COMPONENT OF THE PERIPHERAL STALK) IMPACTS GROWTH, GAMETOPHYTE DEVELOPMENT, AND HEAT STRESS TOLERANCE IN *ARABIDOPSIS THALIANA*

An Honors Thesis

Presented by

Jesse Arsenault

Completion Date:
May 14 2018

Approved By:

_____

Dr. Elizabeth Vierling, Biochemistry & Molecular Biology

ABSTRACT

Title: **Decreased Expression of Mitochondrial ATP Synthase Subunit *d* (a Component of the Peripheral Stalk), Impacts Growth, Gametophyte Development, and Heat Stress Tolerance in *Arabidopsis thaliana***
Author: **Jesse Arsenault**
Thesis/Project Type: **Honors Thesis Seminar**
Approved By: **Dr. Elizabeth Vierling**

As rapid changes in climate continue to threaten global crop yields, a unified model of plant heat stress tolerance is becoming increasingly relevant. Heat stress tolerance in plants involves the coordinated actions of many enzymatic families and is a particularly energy-demanding process. Accordingly, defects in subunits of the mitochondrial F_1F_O-ATP Synthase are known to negatively affect stress tolerance – along with a variety of other functions – in these organisms. We acquired or generated knockout and knockdown mutants of the *d* subunit of ATP synthase (gene name: *ATPQ*) in *Arabidopsis thaliana*, and used these to investigate the large-scale phenotypic significance of that subunit. Total knockout mutants for *ATPQ* are not viable, and heterozygotes possess no visible phenotype, though they transmit *atpq-1* poorly through the female gametophyte and do not transmit it through the pollen at all. Quartet mutant analysis later confirmed this male sterility phenotype. RNAi knockdown mutants of *ATPQ* also display defective and severely slowed growth compared to the wild type and are more sensitive to heat stress. These results indicate that *ATPQ* may play a crucial role in the proper functioning of the mitochondrial ATP synthase holoenzyme, which, when defective, produces wide-ranging faults in energy-demanding cellular processes. With its important structural role established, *ATPQ* further opens the possibilities for research into plant thermotolerance – and specifically into its regulation via mitochondrial enzymes.

Acknowledgments

The past three have been years of tremendous growth – and at times overwhelming struggle. I am indebted to a great many people for my ability to have passed through them and – in the process of doing so – to have helped contribute some small element to the body of scientific knowledge.

I would of course like to thank Dr. Vierling, first for providing me with the opportunity to research at all, and also for her knowledge, guidance, and patience through many, many trials and errors. I would also like to thank Dr. Minsoo Kim, who taught me nearly everything I know about working in a lab, and for his unending positive attitude, patience and assistance day-in and day-out; much of the work in this thesis would not have been possible without his help and hard work. In particular, I want to thank him for his assistance with background information on the project, acquiring materials, generating the RNAi mutants and photographing the mutant quartet pollen.

I would like to thank my friends especially for their seemingly boundless comfort, encouragement, and good humor during this time. And lastly, most importantly, my parents, for their undying love and support throughout the last few years, for which I will always be grateful.

"Nature always strikes back. It takes all the running we can do to remain in the same place."

-René Dubos (Microbiologist, 1901-1982)

"A child said, What is the grass? Fetching it to me with full
hands;
How could I answer the child?....I do not know what it
is any more than he.
I guess it must be the flag of my disposition, out of hopeful
green stuff woven."

-Walt Whitman

Contents

Index of Figures and Tables

Tables

Figures

Abbreviations

ATP – adenosine triphosphate

ATPQ – gene/protein abbreviation for the *d* subunit of ATP synthase

BN-PAGE – blue native polyacrylamide gel electrophoresis

ETC – electron transport chain

HSP – heat shock protein

MS – Murashige-Skoog plant nutrient medium

mTERF – mitochondrial transcription termination factor

NAD^+/NADH – nicotinamide adenine dinucleotide

PCR – polymerase chain reaction

RNA – ribonucleic acid

RNAi – RNA interference

ROS – reactive oxygen species

RT-qPCR – reverse transcriptase quantitative polymerase chain reaction

sHSP – small heat shock protein

TCA – tricarboxylic acid (cycle)

T-DNA – Transfer DNA; DNA inserted into a plant gene from a bacterial source

UPR – unfolded protein response

Chapter 1: Introduction and Literature Review

Section 1: Heat Stress in Plants is a Global Concern

In the face of a rapidly changing climate, agriculturalists are increasingly confronted with the prospect of major crop yield reductions (Figure 1.1). Though plants possess sophisticated cellular mechanisms for coping with stressful environments, the accelerated rate of climate change may outpace these evolved defense strategies, posing a challenge to the maintenance of adequate crop production in the agricultural sector. In France, one climate model was applied to determine the effects of temperature and precipitation on maize yields over the past 50 years. The model concluded that high temperature stress now rivals precipitation in its influence on overall yield (Hawkins et al. 2013). In southeast Asia and the Pacific, a separate analysis of rice yields also concluded that rising temperatures are a detriment to adequate crop yield (Welch et al. 2010b).

Abiotic stresses of all kinds represent a serious threat to agricultural productivity; heat stress, oxidative stress, and other challenging environmental conditions have been shown to decrease crop yields by up to 50% (Boyer 1982). Unfortunately, the problem of global food production also intersects with a concomitant rise in the world's population (United Nations 2017). Current estimates predict that, by 2050, global food production must increase by 59-98% in order to feed an expected population of up to 11 billion people (Valin et al. 2014). To be alleviated, this looming food production crisis demands a rigorous, multifaceted understanding of many relevant fields of study, including the plant abiotic stress response network and its effects on growth and metabolism.

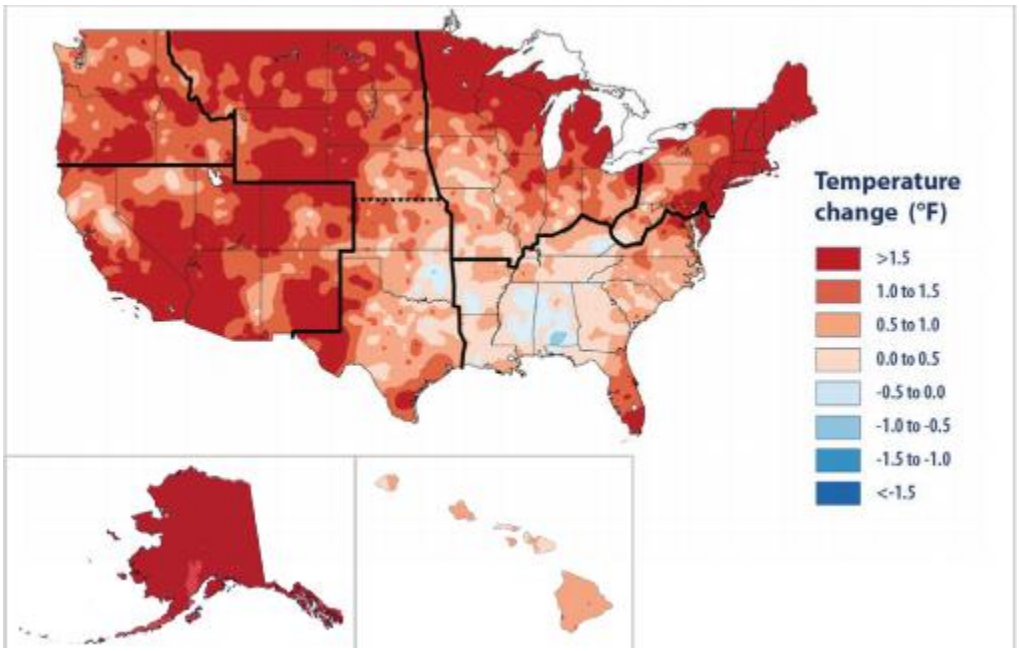

Figure 1.1: Changes in Temperature Across the United States, 1991-2012. Temperature change is expressed relative to the 1901-1960 average for the contiguous U.S., and the 1951-1980 average for Alaska and Hawaii. Adapted from (Melillo et al. 2014).

Heat stress is not a risk to crop yield alone. High temperatures are known to inflict a devastating "diseased state" upon animal cells, denaturing proteins and disrupting tightly regulated signaling pathways (Lavania et al. 2015). Plant cells are equally vulnerable, and pollen grain development is particularly sensitive to high heat (Endo et al. 2009), as are other phases of reproductive development. Heat shock proteins (HSPs), the primary cellular defense response to heat stress, are especially upregulated in developing pollen, reflecting a crossover between reproductive development and abiotic stress (Lavania et al. 2015).

Apart from its effects on reproduction, high temperature stress also disrupts critical metabolic pathways, such as the mitochondrial electron transport chain (ETC). Under heat stress, the ETC produces damaging reactive oxygen species (ROS), which can in turn cause oxidative stress-related damage in the cell (Pucciariello et al. 2012). Conversely, members of the HSP

superfamily confer protection on electron transport proteins in both the mitochondria and the chloroplasts (Hamilton & Heckathorn 2001; Bernfur et al. 2017). In short, reproductive development, energy metabolism, and abiotic stress responses are all highly interrelated in plants.

Though not a crop plant, *Arabidopsis thaliana* is an appropriate model organism through which these interrelated pathways can be studied. *Arabidopsis* is a small flowering plant from the *Brassicaceae* family (Meinke et al. 1998). Favored for its fully sequenced genome, relatively short lifespan, and ease of breeding and mutagenic transformation, *Arabidopsis* is a convenient subject for experiments in flowering plant systems (van Norman & Benfey 2009). Historically, *Arabidopsis* has served as fruitful ground for research into a number of fundamental biological processes. The resulting abundance of *Arabidopsis*-specific literature and experimental protocols, therefore, makes this species ideal for investigations into heat stress resistance, reproductive development, and energy metabolism.

Section 2: Molecular Responses to Heat Stress in Plants

Like most organisms, plants have evolved sophisticated systems for the detection of ambient temperature changes, which can severely impair many aspects of their physiology, from development to reproduction. As sessile organisms, plants are subjected to an even greater demand for adequate heat stress response pathways, as they cannot simply seek shelter when environmental conditions become unfavorable (Mittler et al. 2012). Stressfully high temperatures will denature many proteins, which can obstruct metabolic and signaling pathways and directly trigger the activation of the cellular heat shock response network (Schroda et al. 2015). Though its primary function is to alleviate the effects of heat stress as quickly as possible, this heat stress network also possesses a sort of short-term stress memory known as *acquired thermotolerance*.

Several days after exposure to high heat conditions, the cellular heat stress response system remains activated in case the stressor returns, greatly reducing response time and improving the chances of survival (Baürle 2016). In *Arabidopsis,* such acquired thermotolerance is manifested in the survival of seedlings after exposure to lethal (>45 ºC) temperatures, when conditioned with an initial treatment at nonlethal 38 ºC (Hong & Vierling 2001). As discussed previously, an understanding of acquired thermotolerance and the overall heat stress response in plants is critical to future agricultural development. Long-term shifts in temperature caused by climate change can greatly reduce the yield of major crop plants, even resulting in the sterility of the male reproductive structures (Endo et al. 2009; Lobell et al. 2011).

High-heat conditions can lead to increased fluidity of lipid membranes, RNA and DNA melting, and protein denaturation, all of which may alert plant cells to the presence of temperature stress (Mittler et al. 2012). In the moss model organism, *Physcomitrella patens,* the heat shock response can also be induced by a change in calcium ion flux across the plasma membrane, which may in turn be initiated by increased membrane fluidity (Saidi et al. 2009). Protein denaturation also triggers the heat stress response, along two distinct pathways collectively called the unfolded protein response (UPR). One branch of the UPR begins at the surface of the endoplasmic reticulum (Che et al. 2010) while the other is initiated in the cytosol (Mittler et al. 2012). Cytosolic UPR eventually leads to the activation heat stress master regulator HsfA1a, triggering the downstream expression of several families of cytosolic heat shock protein (HSP) (Figure 1.2; Qu et al. 2013).

The HSP superfamily comprises a diverse assortment of chaperones which are often subcategorized according to their molecular weight. Though characterized as heat-responsive enzymes, HSPs are upregulated in response to multiple stressors including drought and salt

stress, as well as pathogen infection (Breiman 2014). The five main families of HSP are HSP100, HSP90, HSP70, HSP60, and the small HSPs (sHSPs) (Park & Seo 2015). Of these, the sHSP, HSP70, and HSP100 groups are most directly involved in the response to, and recovery from, high-temperature stress (McLoughlin et al. 2016).

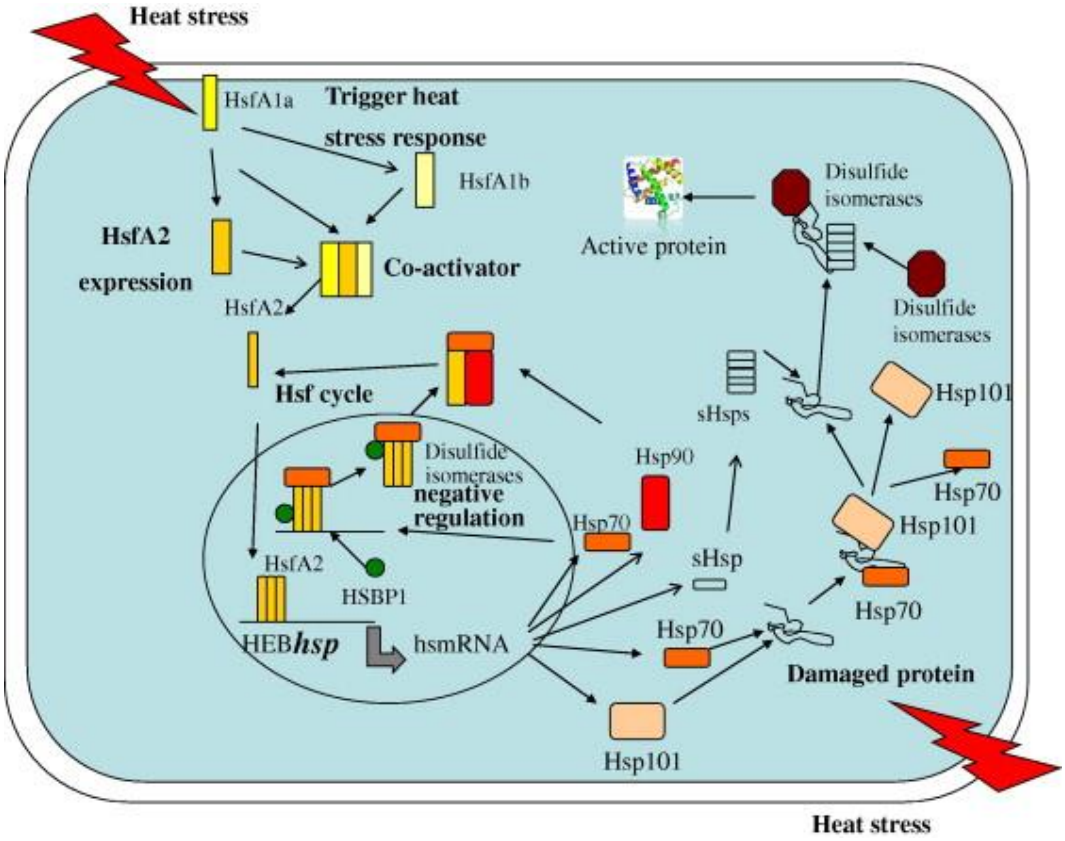

Figure 1.2: General Overview of the Plant Cell's Heat Stress Response Network. Master regulator transcription factors such as HsfA1a and HsfA2 initiate a signaling cascade leading to the expression of a number of response genes, including those of HSP70, HSP101, and the sHSPs. These dynamic enzymes work collaboratively to disaggregate, refold, or assist in the degradation of denatured protein matter. (Adapted from Qu et al. 2013).

HSP70 and HSP100 are ATPases that cooperate during the heat stress response to disaggregate and resolubilize denatured proteins (Figure 1.3; Mogk et al. 2015). HSP70 initiates this coordinated response by binding first to denatured protein aggregates (Acebron et al. 2009). In *E. coli*, HSP100 (also called ClpB) was shown to be recruited by HSP70 (DnaK) via direct

physical interactions between the ClpB M-domain and the ATPase domain of DnaK (Rosenzweig et al. 2013). These interactions further facilitate the disaggregase activity of HSP100/ClpB (Mogk et al. 2015).

HSP100 exists as a hexamer featuring a central pore through which polypeptides are threaded, thus facilitating their disaggregation from the larger insoluble mass (Neuwald et al. 1999). Deletion of yeast HSP100/ClpB (called HSP104) severely decreases the ability of mutants to withstand heat shock (Sanchez & Lindquist 1990). Various mutations in the *Arabidopsis* homolog of ClpB – called HSP101 – have been identified and tend to decrease the ability of mutant plants to acquire thermotolerance. For instance, the mutants *hot1-1* (a E637K point mutation in the second ATP-binding domain) and *hot1-3* (a null T-DNA insertion mutant) cannot acclimate to stressfully high temperatures (Hong & Vierling 2001). Another mutant, *hot1-4*, possesses a similar but dominant negative phenotype – meaning it is sensitive even at 38 ºC – which can be suppressed by a number of intragenic and extragenic mutations (Lee et al. 2005).

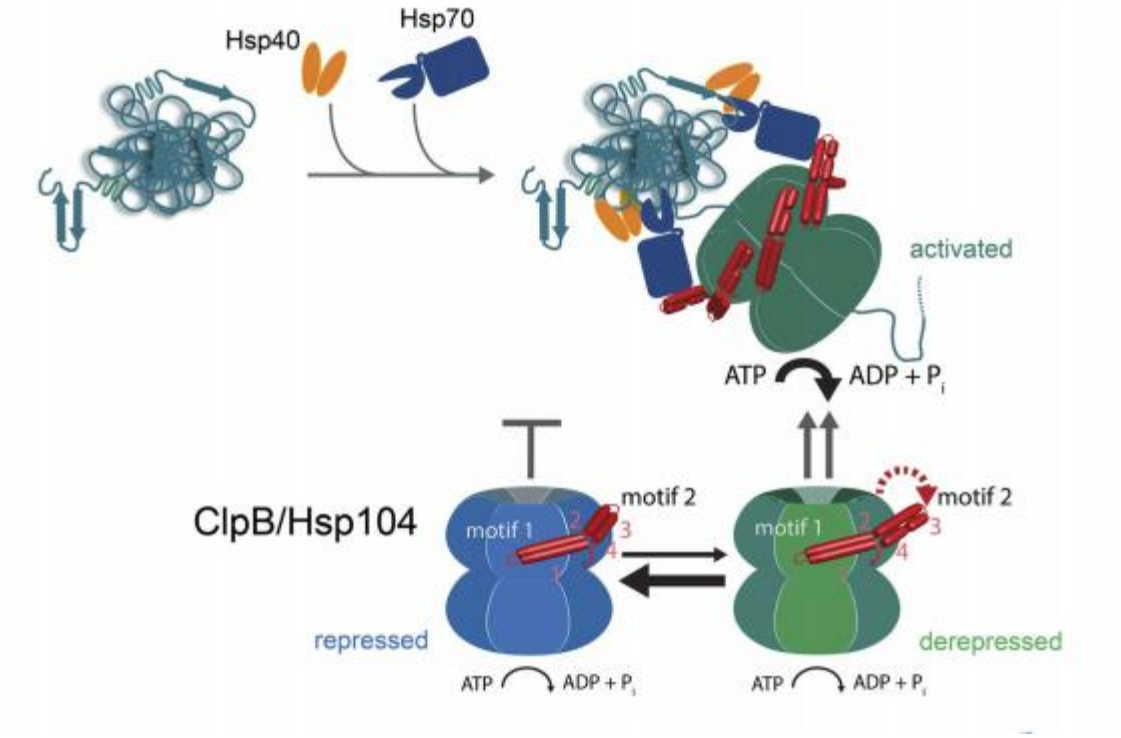

Figure 1.3: HSP70 and HSP100 Cooperate in Many Organisms to Disaggregate Denatured Proteins. Hsp40 and Hsp70 bind first to disaggregated proteins, facilitating the binding and activation of HSP100/ClpB. The HSP100 homolog is activated by the interaction of its M-domain with HSP70, switching it from its repressed to its derepressed state. (Adapted from Mogk et al. 2015).

One extragenic suppressor mutant of the *hot1-4* heat-sensitive phenotype was designated *shot1*. *SHOT1*, the gene in which these suppressor mutations occur, encodes a member of the mitochondrial transcription termination factor (mTERF) family, which is highly diversified in plants (Kim et al. 2012). *shot1-1 and shot1-2*, mutant alleles of the gene, both partially restore the thermotolerance phenotype in the *hot1-4* background, though mutant plants grow slowly and are much smaller at adulthood. However, *shot1-2* was also shown to accumulate ROS at a lower rate and exhibited increased resistance to methyl viologen-induced oxidative stress (Kim et al. 2012). A large-scale proteomics study of *shot1-2* mitochondrial extract also indicated that a number of electron transport-related proteins are downregulated in the *shot1-2* mutant

(unpublished data). Among the first downregulated genes identified in this investigation was *ATPQ*, encoding the *d* subunit of the mitochondrial F_1F_O-ATP synthase holoenzyme, which is the subject of this honors thesis.

Section 3: Pollen Development is a Complex, Closely Regulated, and Energy-Demanding Process

Reproduction is a central function in all forms of life, helping to ensure the survival of the species by transmitting genetic material from one generation to the next and providing opportunities for evolutionary diversity within the population's collective genome. Most plants organize their life cycles according to a model known as *alternation of generations*, characterized by a diploid vegetative stage and a haploid reproductive stage (Host & Reski 2016). Angiosperms such as *Arabidopsis* spend most of their life cycle as large, diploid sporophytes until they are induced to flower, at which point they begin to produce the microscopic haploid gametophytes that participate in reproduction (Horst & Reski 2016).

Angiosperms reproduce sexually using flowers, which are collections of specialized organs that store both the male and female gametophytes. At sexual maturity, the petals of the flower bud (modified leaves that attract pollinating species) open to reveal both the female and male structures, called the carpel and the stamen (Figure 1.4; Suctt & Vandenbussche 2014). Each *Arabidopsis* flower contains one carpel, which stores within it the female gametophyte (including the egg), while the male gametophyte (the pollen grains) develop and proliferate in the anther, at the tip of the stamen (Irish 2009). Pollen grains from the anther make contact with the carpel and extend a single cell – called the pollen tube – into its interior. Once the pollen tube reaches it, a pair of sperm cells fuse with the female gametophyte. The several cells of the female gametophyte, in turn, are fertilized and begin to specialize into an embryo and support structures,

which supply the plant embryo with nutrients (Selinski & Scheibe 2014). Eventually, this process of development will culminate in one of hundreds of dehydrated seeds, kept in biological stasis until environmental conditions signal the initiation of vegetative growth once more.

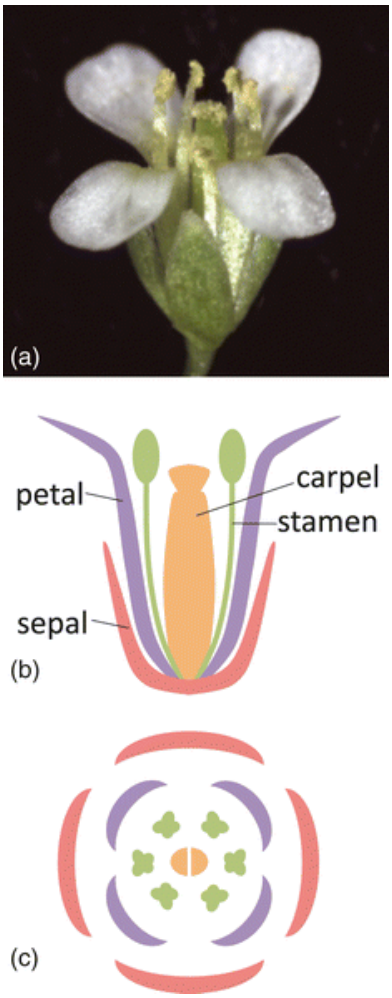

Figure 1.4: Overview of *Arabidopsis* Flower Morphology. All images are of a mature flower. (A) Photograph of flower exterior with all organs visible: green sepals and white petals surround six stamens and two central carpels. (B) Side cross-section diagram of the flower. (C) Top view showing relative orientation of floral organs. Adapted from (Irish 2009).

Pollen development begins well before flowering; it is a highly regulated process, dependent on large amounts of cellular energy and the favorable interactions of several gene regulation pathways. Unlike in animals, any somatic plant cell can theoretically develop into the gametophyte (Gómez et al. 2015). Gametophyte development comes after the development of the anther, which in turn begins with the designation of four archespore cells that will eventually give rise to the anther's four lobes (Gómez et al. 2015). The first archespore division produces a primary sporophytic and primary parietal cell, which will in turn give rise to the pollen mother cells (microsporocytes) and various support tissues, respectively (Figure 1.5; Scott et al. 2004). Included among these support tissues is the tapetum, a metabolite-rich intermediary tissue in developing pollen that is highly sensitive to mutations; many tapetum-related mutations result in male sterility.

Improper destruction of the tapetal layer during pollen development is associated with mitochondrial deficiencies, which are, in turn, frequently linked with male gametophyte lethality (Müller & Rieu 2016). Developing pollen grains derive much of their energy from mitochondria, which helps explain the connection between mitochondrial enzyme deficiencies and defective pollen. For example, knockouts of the plant-specific F_Ad subunit of mitochondrial ATP synthase results in the death of the male gametophyte in *Arabidopsis* (Li et al. 2010). The sunflower homolog of ATP synthase subunit *8* has also been linked with male gametophyte lethality (Hanson & Bentolila 2004). Finally, in pepper (*Capsicum annum.* L.), the genes *orf507* and *Ψatp6-2*, associated with the cytochrome *c* oxidoreductase and F_1F_0-ATP Synthase, respectively, were both associated with anther abortion and the death of the male gametophyte (Ji et al. 2013).

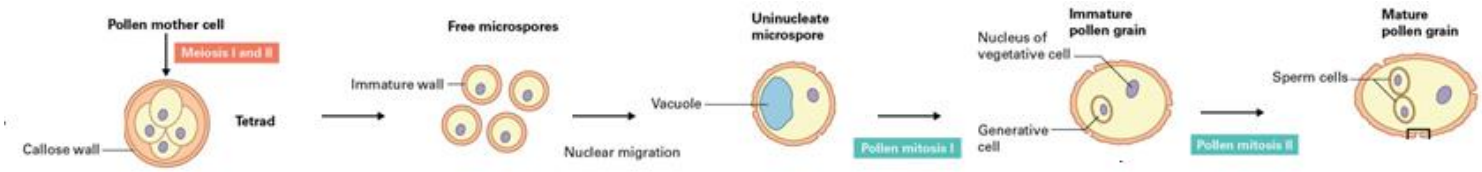

Figure 1.5: Stages of Pollen Grain Development. A pollen mother cell divides by meiosis twice to produce the pollen tetrad (left), which eventually breaks up into individual microspores. Each microspore also undergoes a series of divisions, producing a pair of sperm cells that are carried inside the pollen grain. Upon fertilization, the vegetative cell will extend to form the pollen tube, through which the two sperm cells will travel to reach the egg. Adapted from (Buchanan et al. 2015).

Section 4: The Mitochondrial F_1F_O-ATP Synthase is the Principal Site of ATP Production in the Cell, and is Essential for Many Biological Processes

The mitochondrial ATP synthase (or F_1F_O-ATP Synthase) sits at the terminus of oxidative phosphorylation - the metabolic process by which the cell converts energy from sugars into adenosine triphosphate (ATP) (Gajewski et al. 1986). Energy-rich ATP is considered the principal energy currency of the cell as its hydrolysis releases approximately 30.5 kJ/mol of free energy, which may be used to drive otherwise thermodynamically unfavorable cellular reactions (Gajewski et al. 1986). Oxidative phosphorylation takes place in the mitochondrion, a dual membrane-bound organelle that acts as the primary site of ATP production while also mediating a variety of secondary cellular processes. Mitochondria are usually rod-shaped or spherical, although their shape is highly malleable due to their numerous interactions with other cellular structures as well as with each other (Buchanan et al. 2015). Their two membranes (outer and

inner) give rise to two compartments: the intermembrane space sits between the outer and inner membranes, while the matrix is enclosed by the inner membrane (Figure 1.6, Buchanan et al. 2015). The mitochondrial matrix houses most of the enzymatic machinery for the first phase of oxidative phosphorylation, the tricarboxylic acid cycle (TCA cycle). Products from the TCA cycle are then oxidized at the inner membrane during the second phase, known as the electron transport chain (ETC) (Figure 1.7). Starting with energy-rich pyruvate, these metabolic pathways separate the oxidation of high-energy molecules into a series of minute steps, allowing for a sort of "controlled burn" of the sugar that attempts to maximize free energy extraction in the form of ATP (Junge & Nelson 2015).

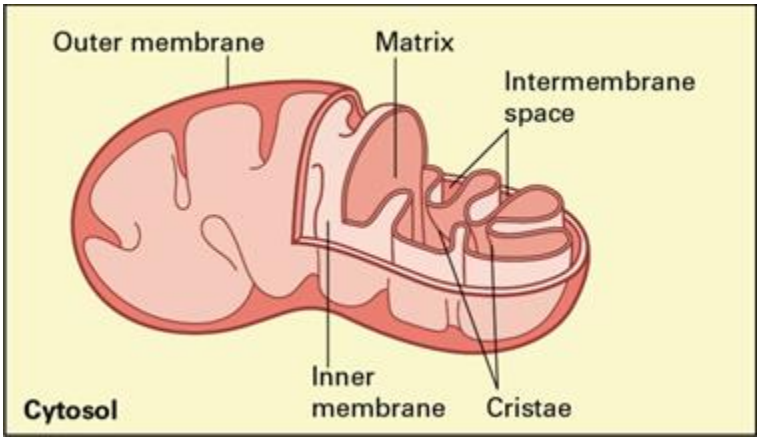

Figure 1.6: Overview of Mitochondrial Structure. Mitochondria can adopt a diverse array of three-dimensional conformations, but their dual-membrane architecture is conserved. The *intermembrane space* is defined between the outer and inner membranes, while the *matrix* occupies the organelle's interior. Invaginations in the inner membrane are called *cristae.* (Adapted from Buchanan et al. 2015)

Mitochondria receive pyruvate – which is itself a product of the cytosolic breakdown of sugars – and import it into the TCA cycle as acetyl-CoA. As it progresses through this series of enzymatic modifications, its released energy (in the form of electrons) is mostly stored in

nicotinamide adenine dinucleotide (NAD^+, NADH when reduced) and flavin adenine dinucleotide ($FAD/FADH_2$). Both these cofactors transfer electrons to the ETC while the oxidized TCA cycle products are recycled and combined with newly imported acetyl-CoA (Buchanan et al. 2015). Although small amounts of ATP are produced by this cycle, the majority of cellular ATP synthesis occurs in the ETC (Buchanan et al. 2015).

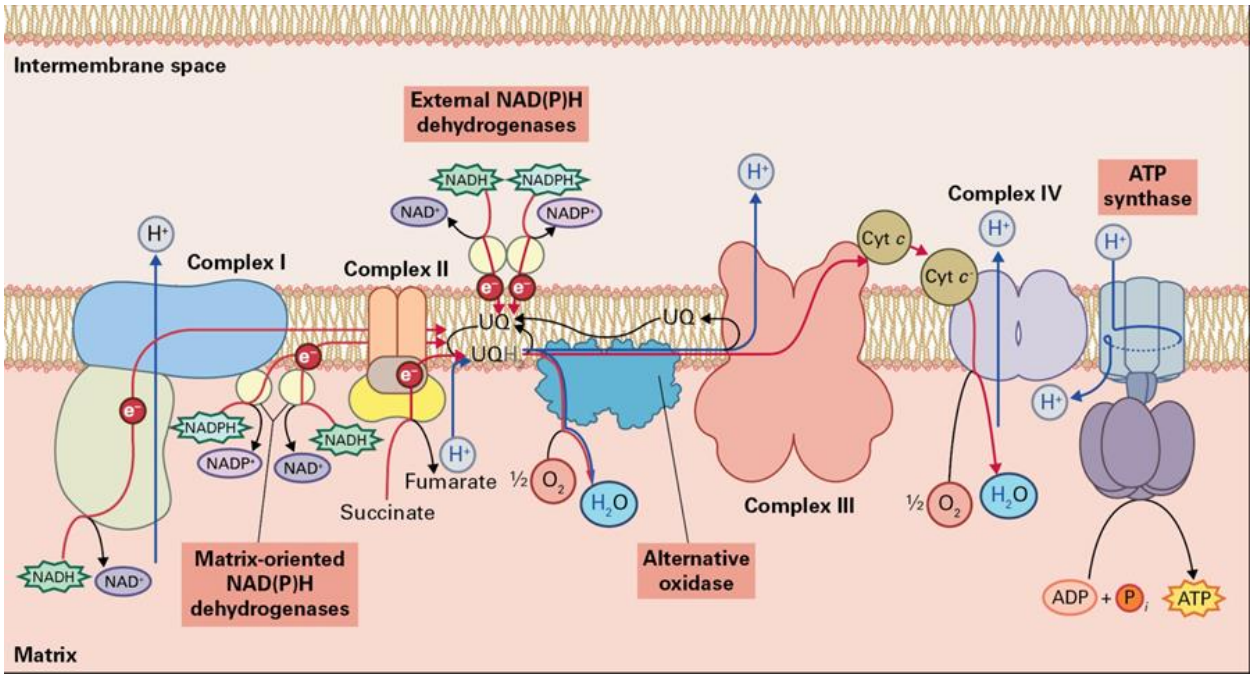

Figure 1.7: Overview of the Plant Mitochondrial Electron Transport Chain. The five major multi-subunit complexes are depicted along with the plant-specific NAD(P)H dehydrogenases and alternative oxidase. Complex V/ATP synthase (right) is embedded in the inner membrane and extends into the mitochondrial matrix. Adapted from (Buchanan et al. 2015).

The ETC comprises a series of five multi-subunit enzyme complexes, along with various proteins and small molecules that reside in or around the inner mitochondrial membrane. These complexes pass electrons sequentially from one to the other while simultaneously pumping protons into the intermembrane space (Junge & Nelson 2015). The resultant buildup of protons in this compartment both acidifies it and increases its positive charge, generating an

electrochemical gradient that can only be resolved by ATP Synthase. This flow of protons through the base of ATP synthase essentially drives the production of ATP (Junge & Nelson 2015).

In general, electrons move through the ETC as follows (Figure 1.7). Electrons are received at complexes I and II from NADH and succinate, respectively. (Complex II, which does not pump protons, also forms part of the TCA cycle, oxidizing succinate to fumarate). Both complexes pass these electrons to the small molecule ubiquinone, which then deposits them at complex III through a sophisticated regenerative cycle. Complex III transfers its electrons to complex IV via cytochrome *c*, and those electrons are ultimately used to reduce molecular oxygen to H_2O, completing the chain. ATP synthase, also known as complex V, helps to reverse the flow of protons initiated by complexes I, III, and IV (Figure 1.7; Junge & Nelson 2015).

The structural organization of ATP synthase itself can be challenging to describe in more than rudimentary detail. This difficulty stems from several factors, including its two greatly divergent functions (proton pumping/rotation and ATP metabolism), its subunit composition (which varies from model species to model species), and a tendency among researchers to try to rigidly subdivide it into non-overlapping subcomplexes with distinct, individual functions. This attempted separation is reflected in its formal name, as F_1 and F_O are used to refer to the soluble/catalytic and structural/proton-pumping subcomplexes, respectively (Welch et al. 2010a). While mostly successful in *E. coli*, which possesses only 8 subunit types, this distinction begins to break down in higher organisms where up to 17+ subunits may exist and play roles in either subcomplex (Capaldi et al. 1999; Junge & Nelson 2015; see also Appendix). Thus, it is usually best to use the *E. coli* enzyme as a model for its structure/function relationships, and then to draw analogies between that enzyme and its relatives in the Eukaryotes.

The *E. coli* ATP synthase subunits are named *α*, *β*, *γ*, *δ*, *ε*, *a*, *b*, and *c* (Figure 1.8). Greek letters refer to subunits of F_1, which includes the catalytic head and the soluble portion of the central rotary stalk. Roman letters refer to the membrane-bound site of proton flow and to the peripheral stalk, which stabilizes the catalytic head (Capaldi et al. 1999). Each ATP synthase holoenzyme consists of three *α* and three *β* subunits, arranged alternatingly into a heterohexamer (Welch et al. 2010a). ATP synthesis (the addition of inorganic phosphate to adenosine diphosphate – ADP) occurs at the junction between the two subunits, and this active site is allosterically modified by the rotation of the central stalk. Within the membrane, protons pass through channels in the *a* subunit, driving the rotation of a ring of *c* subunits (Welch et al. 2010a). This ring is connected to the *γ* and *ε* subunits that make up the rest of the central stalk, the former of which directly interacts with the catalytic head as it spins. Finally, a second, peripheral, stalk extends upward from the *a* subunit. In *E. coli*, this stalk comprises two identical *b* subunits and connects to the catalytic head via subunit *δ* (Capaldi et al. 1999).

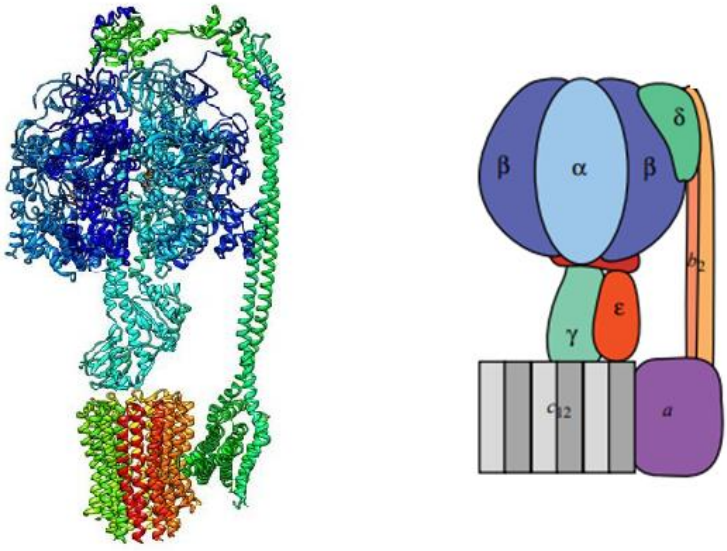

Figure 1.8: The *E. coli* ATP Synthase Structure. Left: crystal structure of autoinhibited *E. coli* ATP synthase (PDB ID: 5T4P) (Sobti et al. 2016). Right: simplified diagram of the *E. coli* ATP synthase holoenzyme (Adapted from Capaldi et al. 1999).

The basic subunit composition of ATP synthase in most Eukaryotes has many similarities, particularly in the F_1 subdomain. The catalytic head is largely the same, as is the central stalk, though the latter consists of three protein subunits instead of two (called *γ*, *δ*, and *ε*). The *a* subunit is joined by an array of membrane-bound peripheral subunits including *A6L/8*, *f*, and *h* (Junge & Nelson 2015). The peripheral stalk, which in *E. coli* consists of two *b* subunits and one *δ/OSCP* subunit, is now made up of four major subunits: *b*, *OSCP*, *F6*, and *d*. These extended proteins wrap around each other to form a flexible peripheral linker between the catalytic head and subunit *a* (Rees et al. 2009). Additional subunits, such as *e* and *g* in yeast, serve more specific functions such as dimerization (Figure 1.9; Wittig & Schägger 2008).

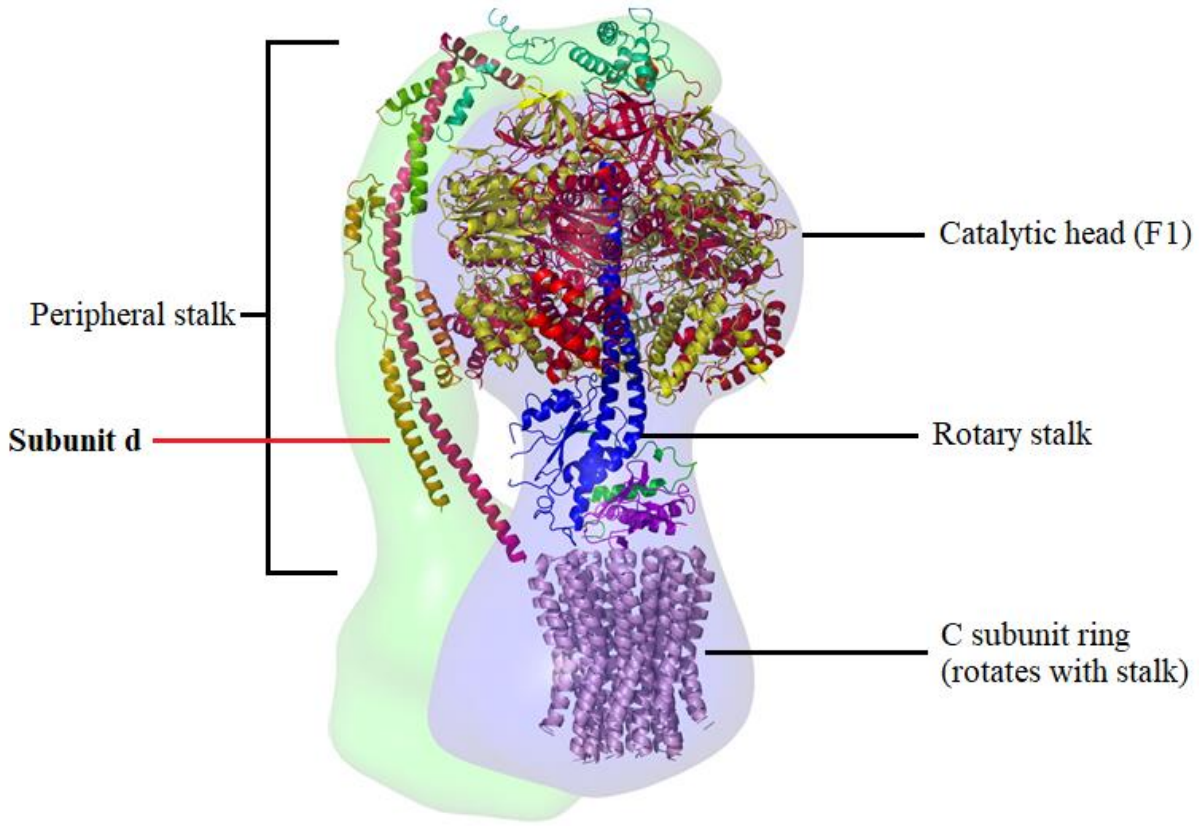

Figure 1.9: Crystal Structure of the Bovine Mitochondrial ATP Synthase. PDB ID: 2WSS. Subunit *d* is depicted in orange/gold as a part of a much more complex peripheral stalk relative to that of *E. coli*. Adapted from Rees et al. 2009.

The aforementioned *d* subunit has been investigated individually in several model organisms but remains largely uncharacterized in plants. One large-scale plant proteomics study, however, indicated that it is upregulated in response to salt stress (Jian et al. 2007). In other organisms, downregulation of this subunit greatly impairs the function of ATP synthase and results in large-scale phenotypic alterations in processes related to metabolic efficiency. RNAi knockdowns of the *Drosophila d* subunit significantly increased oxidative stress tolerance, decreased protein aggregation, and improved lifespans in fruit flies fed a low carbohydrate-to-protein diet (Sun et al. 2014). In humans, knockdowns of the *d* subunit were demonstrated to inhibit the assembly of the holoenzyme (Fujikawa et al. 2015). As a crucial component of an enzyme central to the processes of biological life, additional studies of subunit *d* in plants may yield further insights into the function of this enzyme and its involvement in various biological processes.

Chapter 2: Experimental Methods

Plant Growth Conditions and Materials

All seeds were obtained from the Arabidopsis Biological Research Center (ABRC, at the Ohio State University), except for the *qrt2/qrt2* mutant seeds (SALK_026522C) which were from the Salk Institute for Biological Studies (La Jolla, CA). For growth on plates, seeds were first surface sterilized in 70% ethanol, 0.05% Triton X-100 for 10 min, and then washed under a biological safety cabinet in 100% ethanol. After drying, seeds were sown on square plates of 0.5X Murashige-Skoog medium (plus 0.5% sucrose, 0.8% agarose) prepared according to the manufacturer's directions. BASTA™ selection plates were prepared by adding 0.01% BASTA™ solution to the liquid MS media.

Soil-grown seeds were sown in square pots, arranged in 4 x 8 standard greenhouse trays. Stratification and transfer into growth chambers was performed as described above, with trays being covered during stratification and the first week in the growth chamber.

Segregation Analysis of *atpq-1*

Plants heterozygous for *atpq-1* were allowed to self-fertilize and seeds were grown on soil for genotyping. Genomic DNA extraction was performed on collected F1 leaf tissue samples according to Sika et al. 2015. Several differences from this protocol should be noted: the extraction buffer was 200 mM Tris-HCl (pH 7.5), 250 mM NaCl, 25 mM EDTA, and 0.5% SDS. The extracted DNA was resuspended in 0.1X TE Buffer (10 mM Tris-HCl pH 8.0 and 1 mM EDTA) instead of sterile water.

The gene was amplified via PCR using three primers (two for the wild type allele and one for the T-DNA insertion) (See Appendix). Because the gel results were unclear when all 3 primers were used at once, the PCR was performed twice, once using forward and reverse *ATPQ* primers and again using the forward *ATPQ* primer and the T-DNA reverse primer. The wild type amplicon size was expected to be 957 bp. The *atpq-1* mutant amplicon size was expected to be approximately 500 bp. PCR results were visualized on a 1.2% agarose gel under UV light, and the number of homozygous and heterozygous plants was recorded.

Bioinformatics and Protein Structure Prediction

The amino acid sequence for ATPQ (Locus no. At3g52300) was retrieved from The Arabidopsis Information Resource (TAIR), while homologs from *G. max*, *A. lyrata*, *Z. mays*, *H. vulgare*, and *O. sativa* were identified and retrieved from UniProt (www.uniprot.org). Sequences were compared using Clustal Omega (https://www.ebi.ac.uk/Tools/msa/clustalo/). ATPQ structure prediction was performed using the Protein Homology/analogY Recognition Engine (PHYRE) version 2.0 on "intensive" setting. Transit peptide prediction was performed using the TargetP 1.1 server (Technical University of Denmark Dept. of Bio and Health Informatics, www.cbs.dtu.dk/services/TargetP) on "Plant" and "No Cutoff" settings.

Generation of *atpq-1*/+ Quartet Mutants

Two crosses were made between *atpq-1* heterozygotes and *qrt2/qrt2* mutant plants (SALK_026522C, see above), the genotypes of which were confirmed with PCR (for primer sequences, see Appendix). Following the beginning of growth stage 6.00, unopened flower buds were selected from *qrt2/qrt2* plants for pollen donation. Unopened buds from *atpq-1*/+ plants

were dissected such that only the stigma remained. Pollen was transferred by direct contact with the anthers of *qrt2/qrt2* flowers. The selected stigmas were marked and upon desiccation the siliques were harvested.

Pollen Microscopy

Using forceps, anthers from *atpq-1/+* x *qrt2/qrt2* were dissected out of selected Stage 6.30 flowers, visualized, and photographed under a light microscope.

Generation of RNAi Knockdowns

Note: The generation of the RNAi mutants was kindly performed in its entirety by Dr. Minsoo Kim, according to the following protocol: A 300 bp *ATPQ* fragment was amplified (see Appendix for primer sequences) with primers ATPQ-F4 and ATPQ-R4 and cloned into the pENTR/D-TOPO vector, resulting in pMK118.

Using pMK118 as a template, the *ATPQ* fragment with restriction enzyme sites was amplified with primers ATPQ-F5 and ATPQ-R5. The PCR fragment and vector pFCG5941 were digested with AscI and SwaI and ligated together to make pMK124. The same PCR fragment and pMK124 were digested with BamHI and XbaI and ligated together to make pMK127.

pFGC5941 (the empty vector for RNAi construct) and pMK127 (the *ATPQ* RNAi construct) were transformed into *Agrobacterium tumefaciens* GV3101. Transformation of Col-0 plants with the constructs were performed by the floral dip method (Clough & Brent 1998) and BASTA-

screened as described above.

Growth Phenotyping of RNAi Knockdown Mutants

BASTA-screened T3 seeds (*RNAi:ATPQ1-5*) were sown on soil as described previously. Three seeds were sown per pot and a total of 24 seeds per line were sown. Col-0 and RNAi empty vector (FGC5941.1.8) seeds were grown as well. Mutant plants were photographed beside control plants at various points in their life cycles, for visual comparison.

Heat and Oxidative Stress Assays

Seeds were sterilized in 50% bleach, 0.05% Tween-20, washed 4 times with sterile water, and plated in straight lines on 10-15 mL MS media. For the heat stress assay, after 2.5 days stratification at 4 ºC, plates were wrapped in foil and grown vertically in the dark for 2.5 days, so that the hypocotyls extended parallel to the MS media. For the oxidative stress assay, plates were grown vertically for four days and then seedlings were transferred to new plates: non-stress control seedlings were transferred to standard MS plates, while the seedlings to be stressed were transferred to plates of MS + 50 nM methyl viologen. Root lengths were marked, and then allowed to grow for three more days before final root measurements were taken.

After 2.5 days, heat stress assay plates were placed in a 38 ºC incubator for 1.5 hours and then allowed to recover at room temperature for 2 hours. The same plates were next moved to a 45 ºC incubator for either 2.5 or 3 hours. The length of the hypocotyl (measured as the intersection of the cotyledons) was marked on the plate, and the plates were grown vertically in the dark for an

additional 2.5 days, at room temperature. The new position of the hypocotyl was marked again, and individual hypocotyl lengths were measured using a loupe equipped with a millimeter ruler.

The mean hypocotyl length was calculated for each line at room temperature, while hypocotyl lengths for heat-shocked lines were expressed as decimal fractions of the mean length at room temperature for each line. The same calculation was performed for the oxidative stress assay, except using root lengths rather than hypocotyl lengths.

Chapter 3: Results

ATPQ Knockout Mutants are Non-Viable in Arabidopsis, and Heterozygotes Have Impaired Transmission of the Mutant Gene Across Generations

In order to investigate the biological role of *ATPQ* (locus: At3g52300), heterozygotes for a T-DNA knockout mutant (*atpq-1*, or SAIL_97_F05.V1) were acquired and allowed to self-fertilize to produce F1 offspring (here, *atpq-1* refers to the mutant allele; *atpq-1*/+ refers to the heterozygote). *ATPQ* is a 2021bp gene consisting of five exons and four introns; the T-DNA insertion in *atpq-1* is a knockout insertion within the second intron. The gene encodes a 168-amino acid, 19.6 kDa protein which is predicted to contain several α-helical domains and which is well-conserved in the higher plants (Figure 3.1A-C). TargetP analysis of the amino acid sequence did not predict a transit peptide targeting the mitochondrion (Figure 3.1D). Because the F1 generation was produced by self-fertilizing *atpq-1* heterozygotes (*atpq-1*/+), a Mendelian genotypic ratio of 1:2:1 was expected (+/+ : *atpq-1*/+ : *atpq-1/atpq-1*). A sample of 29 F1 plants was chosen for genotyping, and genomic DNA extraction was performed on leaf samples from each, followed by three-primer PCR to detect the *ATPQ* gene and the T-DNA insertion.

Contrary to expectations, the genotypic ratio of the F1 progeny was approximately 3:1:0, a non-Mendelian ratio with no homozygous mutants (Table 3.1). In spite of this fact, the growth phenotype of *atpq-1*/+ is indistinguishable from that of the wild type (data not shown). Additionally, the bias toward the wild type genotype indicates that the *atpq-1* allele

may be poorly transmitted through one or both gametes, although from these data alone it is impossible to predict whether – or how – this occurs in the mutant.

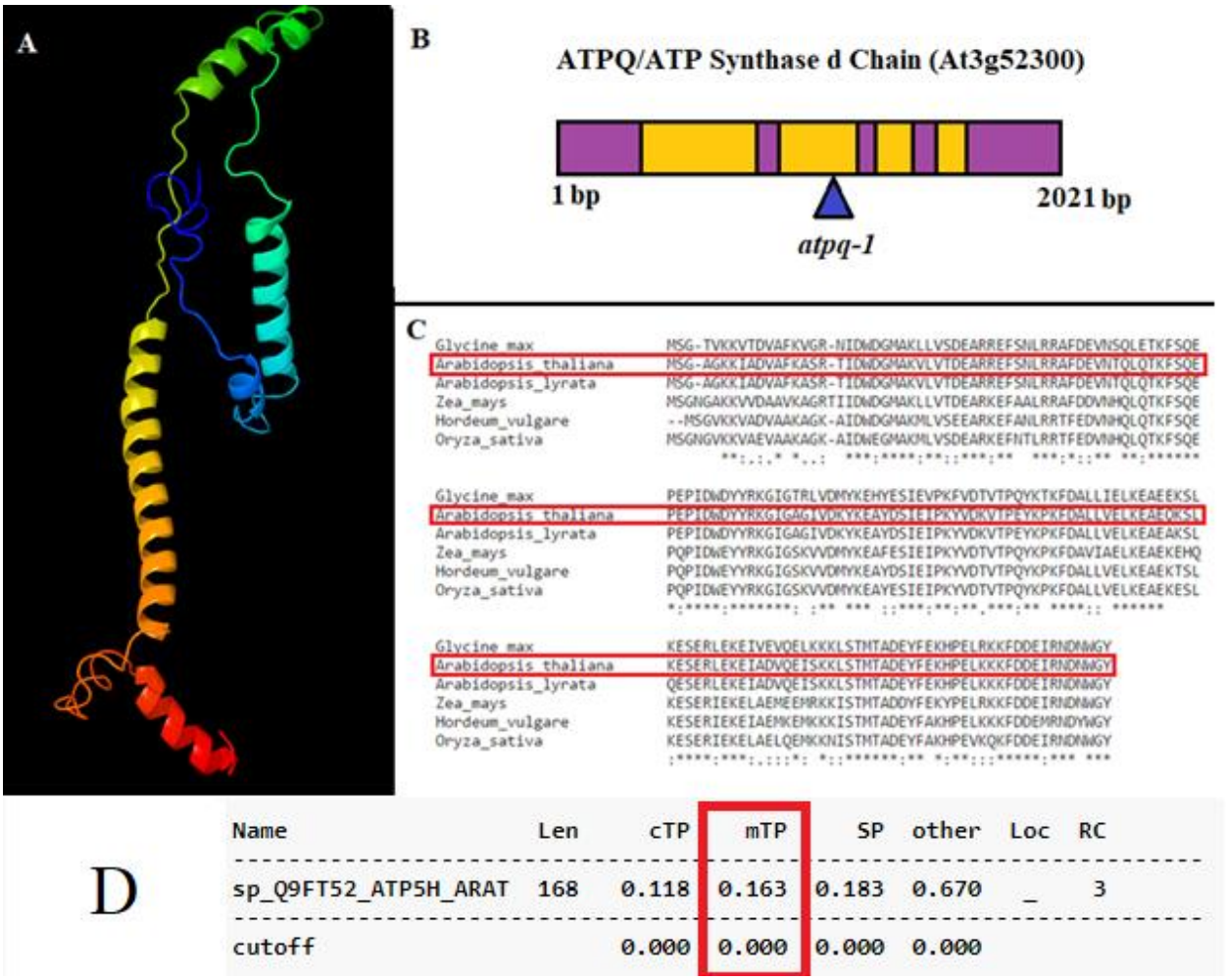

Figure 3.1: Overview of ATPQ in *Arabidopsis*. (A) PHYRE2 prediction of ATPQ structure. Colored blue to red: N- to C-terminus. (B) Gene map of *ATPQ* (At3g52300). Exons are in purple, introns are in yellow, colored bar sizes to scale. The blue arrow represents the site of the *atpq-1* T-DNA insertion. (C) Clustal Omega amino acid sequence alignment of *Arabidopsis thaliana* ATPQ (red box) against homologs from other representative higher plant species. See Appendix for homolog accession numbers. (D) TargetP prediction for the presence of a transit peptide (mitochondrial prediction in red box). Higher scores indicate higher likelihood of a targeting peptide for that compartment. cTP = chloroplast, SP = secretory pathway. RC is the reliability class, the rank of the difference between the highest and lowest prediction scores, 1 being strongest and 5 being weakest.

atpq-1 is not transmitted through the male gametophyte and is poorly transmitted through the female gametophyte

The effect of *atpq-1* on both gametophytes can be identified by backcrossing F1 heterozygotes with wild type members of the parental generation. 13 independent backcrosses were performed (6 using a heterozygote male and 7 using a heterozygote female) and progeny from each cross were genotyped as described above. If the haploid gametophytes were unaffected by *atpq-1*, a 1:1 genotypic ratio of wild type to heterozygous progeny would be expected. For both sets of crosses, however, this ratio was significantly skewed toward the wild type, indicating that male and female gametophytes lacking ATPQ have difficulty with gametophyte development and/or fertilization.

More specifically, in the female heterozygote-based crosses, only 18.03% of the progeny possessed the *atpq-1* allele, a genotypic ratio of almost 4:1. The male heterozygote crosses were even more severe; 100% of the progeny from these crosses were wild type, with no transmission of the mutant allele (Table 3.1). This indicates that pollen grains carrying the *atpq-1* allele are effectively sterile, and either do not develop properly or cannot successfully fertilize the egg.

Table 3.1: Genotypic ratios of *atpq-1*/+ self-crossed progeny (F1) and reciprocal backcrosses using male and female heterozygotes. Percent of total sample per genotype is given in parentheses. The expected Mendelian ratio for the F1 self-cross was 1:2:1. Expected ratio for the backcrosses was 1:1.

Generation	No. Wild Type (%)	No. Heterozygous (%)	No. Homozygous Mutant (%)
F1 (het x het) (n = 29)	22 (75.96%)	7 (24.14%)	0 (0%)
Backcross: Male het (n = 106)	106 (100%)	0 (0%)	0 (0%)
Backcross: Female het (n = 120)	100 (81.97%)	22 (18.03%)	0 (0%)

Pollen tetrad analysis in the *qrt2/qrt2* background confirms that male gametophyte development is impacted by *atpq-1*

To more fully explore the effects of *atpq-1* on male gametophyte development, *atpq-1*/+ plants were crossed into the quartet mutant (*qrt2/qrt2*) background (seed line: SALK_026522C). *QUARTET2* (*QRT2*) encodes a polygalacturonase in *Arabidopsis* that, when knocked out, inhibits the separation of developing pollen grain tetrads (Ogawa et al. 2009). These tetrahedral arrangements of haploid cells can be visualized under a microscope and, because they descend from the same mother cell, will each possess either the wild type or *atpq-1* allele in a 1:1 ratio. If a mutant allele negatively impacts development, there will often be visible defects in the affected cells.

Figure 3.2: Exemplar Pollen Tetrad Collected From an *atpq-1/+* x *qrt2/qrt2* Mutant. Red arrows indicate small, deformed pollen grains. Image was photographed under a light microscope. (Courtesy of Dr. Minsoo Kim)

Two independent crosses of *atpq-1/+* into the *qrt2/qrt2* background were prepared, and seeds from the selected siliques were grown on soil until they began producing flowers. The presence of the *atpq-1* T-DNA insertion was confirmed in the progeny as described above, and PCR was similarly used to detect the *qrt2* T-DNA insertion, as a confirmation of the success of the crosses. Pollen was isolated from the anthers of open flowers and visualized under a confocal microscope. Pollen grains from the *atpq-1*-containing plants exhibited slowed growth and deformities in 2 of the 4 tetrad cells, compared to wild type (Figure 3.2).

RNAi knockdowns of *ATPQ* have an impaired growth phenotype

Because *ATPQ* is an essential gene (Table 3.1), homozygous knockout mutants are not possible in *Arabidopsis*. To more clearly determine the effect of the absence of ATPQ in *Arabidopsis*, we generated several independently transformed RNAi knockdowns of *ATPQ*. As the transformation contains a BASTA™ (glufosinate) resistance gene, herbicide screening was performed across several generations to identify plants that were homozygous for the transformation (characterized by 100% BASTA resistance among seedlings in the T3 generation). Of the identified RNAi lines, five were selected for study from 5 independent T1 transformants (here called *RNAi:ATPQ1-5*).

24 seeds from each RNAi knockdown line, wild type (Col-0), and an empty vector control line (FGC5941.1.8) were sown on soil. Over the following weeks, the growth phenotype of the plants was monitored and representative photographs were taken at various points of development (Figure 3.3). RNAi knockdown mutants consistently displayed severely slowed growth, as well as malformed leaves and flowers – featuring irregular or "crinkled" edges and abnormal sizes compared to those of the wild type (Figure 3.3). In general, knockdown plants grow extremely slowly in comparison to the wild type. Most have small, shriveled leaves, short stems, and misshapen flowers and floral organs.

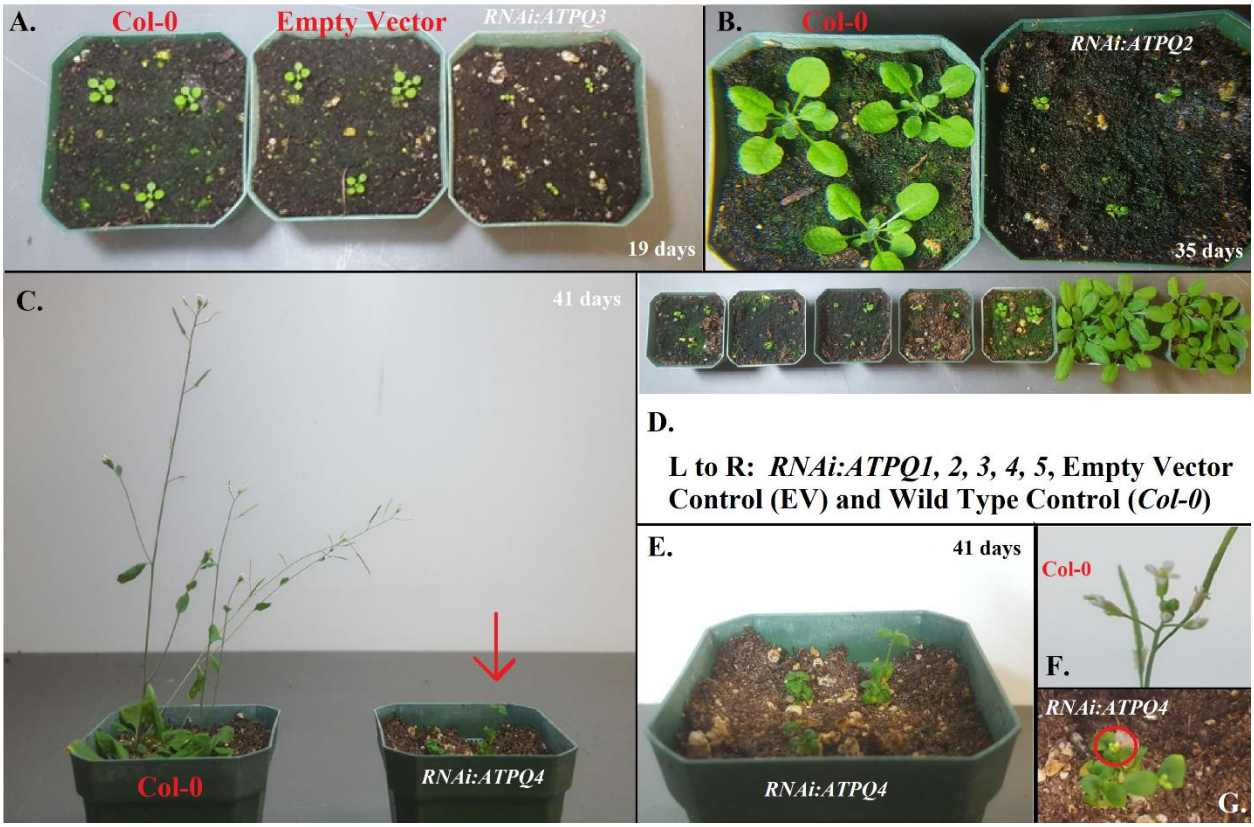

Figure 3.3: Growth Phenotype Differences Between Wild Type, Empty Vector, and RNAi Knockdown Mutants. All plants were grown under long day conditions (16h light, 8 h darkness). Different lines are photographed in different pictures to demonstrate consistent slow growth of knockdown mutants regardless of mutant line. (A) Side-by-side comparison of 19-day-old Col-0 control, EV control, and *RNAi:ATPQ*3 plants. (B) Side-by-side comparison of 35-day-old Col-0 and *RNAi:ATPQ4* plants. (C) 41-day-old Col-0 and *RNAi:ATPQ2* plants. Red arrow indicates the shoot of one of the RNAi mutants. (D) Side-by-side comparison of all knockdown lines and control plants (labeled), X days old (E) Detail of 41-day-old *RNAi:ATPQ2* plants. (F, G): Flower/bud comparison between 41-day-old Col-0 and *RNAi:ATPQ2* plants (flower circled in red).

ATPQ knockdowns are more sensitive to heat

The thermotolerance phenotype of the *RNAi:ATPQ* lines was determined by exposing dark-grown seedlings, grown in a straight line, to temperatures of 38 ºC and 45 ºC with a 2 hour recovery period at room temperature (22 ºC; Hong & Vierling 2001). The length of the

hypocotyl was marked immediately after heat shock and then re-measured after 2.5 more days of growth in the dark. An additional set of plates was grown at room temperature as a control, and Wild Type (Col-0) and heat-sensitive (*hot1-3*) plants were also assayed as a positive and negative control.

All five *RNAi:ATPQ* lines had significantly shorter hypocotyls after heat stress compared to Wild Type. Whereas Col-0 plants grew 6-7 mm after heat stress, the average hypocotyl extension of the RNAi knockdowns was between 4-5 mm, approximately 50% of the unstressed length (Figure 3.4). Wild type and empty vector controls grew consistently at 70-80% of room temperature growth after heat stress at both time points. Alternatively, *RNAi:ATPQ5* showed significant sensitivity to heat stress after 3 hour exposure, though without quantification of each line's knockdown severity it is impossible to determine the cause of this sensitivity.

Table 3.2: Average *RNAi:ATPQ* Hypocotyl Elongations After No Heat Stress, 2.5 hours Heat Stress, and 3 Hours Heat Stress. Values were used to create the graphs in Figure 3.4. *hot1-3* is a heat-sensitive negative control, FGC4956.1.8 is an empty vector control for the RNAi knockdown mutants. Number of seeds used to calculate each average is given in brackets [n].

Genotype	Average Hypocotyl Elongation (Room Temperature) (mm) [n]	Average Hypocotyl Elongation (2.5 Hrs Heat Stress) (mm) [n]	Average Hypocotyl Elongation (3 Hrs Heat Stress) (mm) [n]
Wild Type (Col-0)	7.1 [17]	5.8 [16]	4.6 [17]
hot1-3	6.0 [12]	1.1 [12]	0 [12]
Empty Vector (FGC4956.1.8)	7.6 [13]	5.5 [15]	5.3 [18]
RNAi:ATPQ1	5.7 [14]	3.1 [15]	2.7 [13]
RNAi:ATPQ2	6.9 [18]	3.6 [16]	3.0 [16]
RNAi:ATPQ3	7.3 [16]	3.3 [14]	3.1 [15]
RNAi:ATPQ4	7.1 [11]	3.4 [12]	2.9 [14]
RNAi:ATPQ5	7.1 [11]	3.4 [18]	2.4 [14]

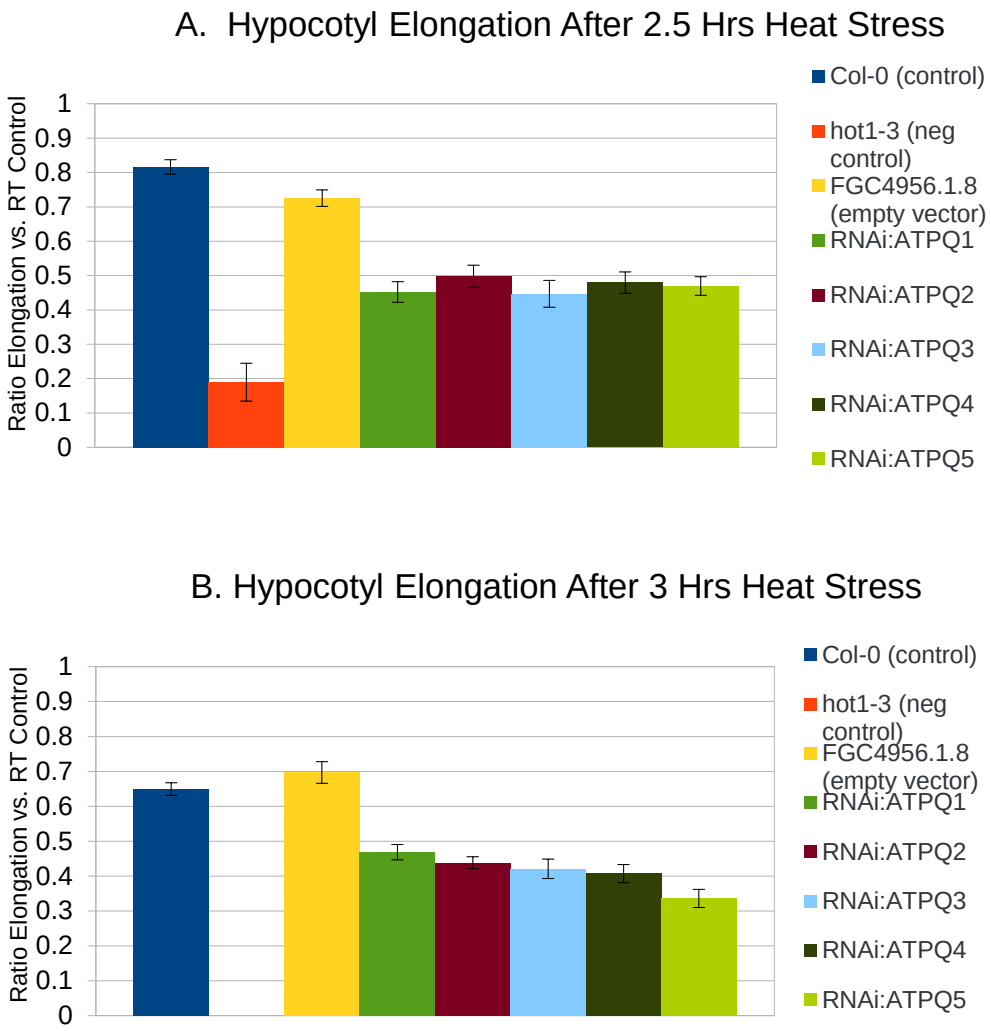

Figure 3.4: Hypocotyl Growth of RNAi Knockdown Mutants After Heat Stress, Relative to Non-Stressed Growth. Heat-acclimated, plate-grown seedlings were exposed to 45 ºC for either 2.5 (A) or 3 (B) hours. Col-0 and RNAi empty vector seedlings served as positive controls, and heat-sensitive *hot1-3* seedlings served as negative controls. Hypocotyl lengths for

2.5 days after heat stress are expressed as ratios to the average room temperature hypocotyl growth for the same period of time. Bars indicate standard error.

RNAi:ATPQ plants seem to have varied responses to oxidative stress

Along with the heat stress assay, *RNAi:ATPQ* seedlings were also grown on MS and MS + 50 nM methyl viologen plates for one week. Root elongation on the methyl viologen plates between days 4 and 7 was measured and compared with the average root elongation of non-stressed seedlings during the same time. Only one of the *ATPQ:RNAi* lines showed significantly different root elongation compared to the wild type and empty vector controls; *ATPQ:RNAi3* grew much more slowly than the positive controls (only approximately 25% of unstressed *ATPQ:RNAi3*, compared to 40% in the wild type). However, there may be confounding factors to this data (see Discussion).

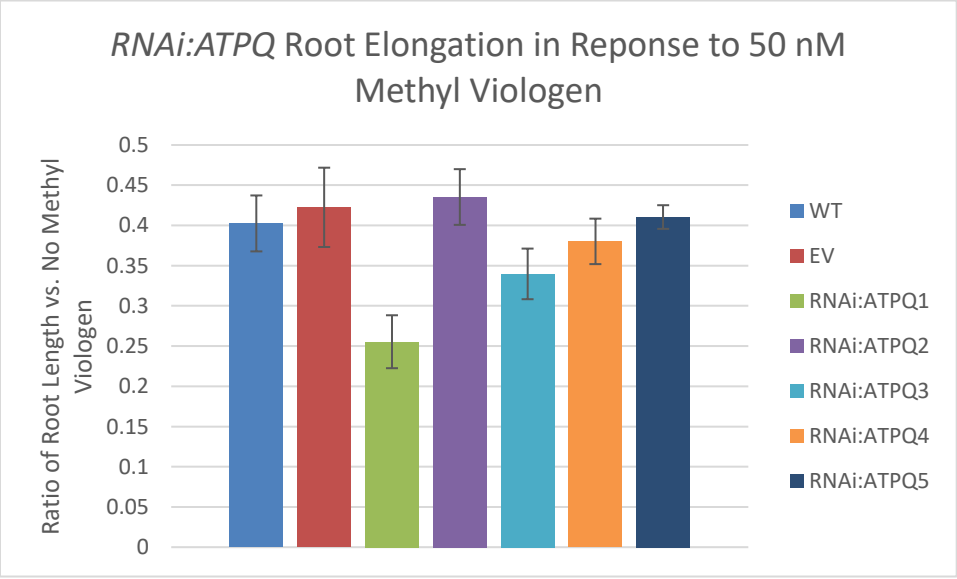

Figure 3.5: Oxidative Stress Response in *RNAi:ATPQ* Mutants. Error bars indicate standard error. WT = Col-0 wild type control. EV = FGC4951.1.8 empty vector control. Values indicate average 3-day root elongation for each line divided by average 3-day root elongation in the absence of methyl viologen.

Table 3.3: Average Root Elongation Lengths of Stressed and Non-Stressed *RNAi:ATPQ* Mutants During Oxidative Stress Assay. The sample size for each average is provided in brackets [n]. The ratio of average elongation under stress to average elongation under no stress was used to produce the graph in Figure 3.5.

Genotype	Average Root Elongation (MS, No Methyl Viologen) (mm) [n]	Average Root Elongation (MS + 50 nM Methyl Viologen) (mm) [n]
Wild Type (Col-0)	11.8 [9]	4.7 [19]
Empty Vector (FGC4956.1.8)	7.7 [11]	5.0 [12]
RNAi:ATPQ1	8.4 [13]	3.0 [15]
RNAi:ATPQ2	9.8 [15]	5.1 [17]
RNAi:ATPQ3	9.7 [13]	4.0 [16]
RNAi:ATPQ4	10.5 [11]	4.5 [13]
RNAi:ATPQ5	11.9 [15]	4.8 [16]

Chapter 4: Discussion and Conclusions

Control mechanisms of plant growth, reproductive development, and the abiotic stress response all coalesce around the supply of cellular energy – ATP. When this supply is disrupted or decreased, the resultant slowdown of cellular chemical reactions can be an inconvenience at best, and fatal at worst. As the primary site of ATP production in the cell, ATP synthase is itself a critical junction between these processes, and deficiencies in ATP synthase architecture have been shown to negatively impact a broad spectrum of processes in various model species (Sun et al. 2014, Li et al. 2010). This thesis attempts to further probe the relationship between these disparate processes via the *d* subunit of the plant mitochondrial holoenzyme in particular.

ATP synthase subunit *d*, encoded by the gene *ATPQ*, is an essential gene that produces a normal growth phenotype in plants heterozygous for its knockout allele (*atpq-1*) but severely impairs growth when its expression is partially inhibited by RNAi (Table 3.1). Transmission of *atpq-1* through the gametophytes is also impaired – partially in the female and totally in the male (Table 3.1). Further investigations into the development of the male pollen grain in *atpq-1* heterozygotes revealed that two of the four pollen grains per tetrad are small and deformed (Figure 3.2). Finally, RNAi knockdowns of *ATPQ* consistently impair acquired thermotolerance relative to the wild type, reinforcing the connection between cellular energy architecture and the abiotic stress response (Figures 3.3, 3.4).

The results of the oxidative stress assay were less clear than those of the heat stress assay (Figure 3.5, Table 3.3), but several factors specific to this experiment may indicate that the data presented may not accurately represent the response of these mutants to oxidative stress. For instance, the standard error is notably wide for almost every genotype, indicating less consistency in growth from seedling to seedling even within a shared mutant line. It is also

unexpected that only one knockdown mutant should be significantly sensitive, while the others are not – a more expected result would resemble that of the heat stress assay, in which the five knockdown lines have similar phenotypes. It is possible that, because of the assay's reliance on root measurements, the extension of some roots was impaired by other seedlings in their path, skewing the average length of elongation. There may have been an issue with the oxidative stress plates as well; methyl viologen may have been unevenly distributed in the media due to some unforeseen complication, for example. As such, a repetition of this assay is strongly encouraged before any conclusive statements can be made about the response of *RNAi:ATPQ* mutants to oxidative stress.

Deficiencies in individual ATP synthase subunits can have disastrous large-scale effects on the mutant organism. In *Arabidopsis*, knockdown mutants of the δ subunit (part of the rotary stalk, F_1 subdomain) produced impaired male gametophyte development and impaired metabolic functioning, among various other -largely negative – effects (Geisler et al. 2012). Similarly, the plant-specific *F_Ad* subunit causes male gametophyte sterility in *Arabidopsis* knockout mutants (Li et al. 2010). In *Drosophila*, knockdown mutants of the *d* subunit show increased resistance to oxidative stress and pronounced changes in metabolic rationing (Sun et al. 2014; see also Ch. 1 S. 4). If ATP synthase subunits are sufficiently similar across organisms, an explanation for this phenomenon may be found in studies of human subunit *d* knockdowns. The human homolog, *ATP5H*, was knocked down in HeLa cells to examine its effects on the assembly of the F_1F_O-ATP Synthase. It was determined that, in the relative absence of subunit *d*, the enzyme complex could not successfully assemble and instead existed as a pair of separate, partially assembled substructures – the F_1-*c*-ring and the *b*-*e*-*g* complex (Fujikawa et al. 2015; Figure 4.1). A similar

breakdown in ATP synthase assembly could be occurring in these *Arabidopsis* mutants, resulting in a potentially devastating drop in ATP production and overall cellular performance.

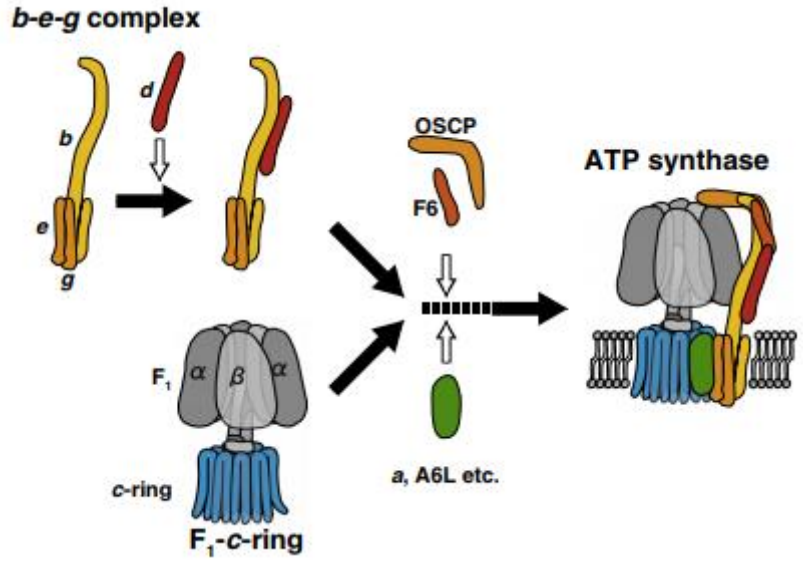

Figure 4.1: **Proposed assembly model for the human F_1F_O-ATP synthase**. The *d* subunit is predicted to join the peripheral stalk complex after subunits *b*, *e*, and *g*, while F_1 assembles largely independently (Adapted from Fujikawa et al. 2015).

As discussed in Chapter 1, gametophyte development, stress tolerance, and growth are all extremely energy-demanding processes. Mutations that impact the production of ATP can interfere with energy-critical phases of development (or day-to-day operation, as in the heat stress response) (Boyer 1982). Therefore, it is quite possible that a lack of sufficient ATP is responsible for the phenotypes observed during this project. This does not, however, answer the question of *how* these processes are specifically linked, and precisely how the mitochondrion helps to orchestrate the plant abiotic stress response or the multi-stage development of pollen.

Disturbances in ETC function have broad ramifications due to the interconnected nature of its constituent complexes. Oxidative stress-inducing ROS are produced at the ETC complexes in response to a variety of stressors, including heat (Qu et al. 2013) and nitric oxide (NO) (Scheler et al. 2013). While the proton gradient that spans the inner membrane can be alleviated in plants via the alternative oxidase (AOX), much of its equilibrium is due to the action of ATP synthase (Buchanan et al. 2015); a removal or disruption of that enzyme could greatly diminish effective ETC flow and, by extension, the stress responses mediated by the ETC elements.

The crucial role of tapetal breakdown during pollen development has also been discussed previously (Ch. 1, S. 3). Such a process is one of several during pollen development that draws on immense concentrations of ATP to reach completion. And completion of this stage is essential to pollen survival – ATP synthase deficiencies are known to cause incomplete breakdown of the tapetum and, by extension, pollen abortion (Ji et al. 2013). If the F_1F_O-ATP Synthase is only undergoing partial assembly in the *atpq-1* and *RNAi:ATPQ* mutants, the resultant diminished ATP concentration may impair the plants' ability to complete this step of pollen growth.

The results of this study indicate the importance of the *d* subunit in *Arabidopsis* ATP synthase, but there are still many aspects of its importance – as well as that of the entire complex – to be elucidated. For instance, a similar experiment to that of (Fujikawa et al. 2015), employing BN-PAGE and western blotting, could be used to determine the ATP synthase assembly phenotype in mutant *Arabidopsis*. Total ATP production could also be assayed (e.g. with a luciferin-luciferase kit) to confirm the negative impact of *ATPQ* knockout/knockdown on cellular energy production.

Another potentially useful step would be the analysis of *RNAi:ATPQ* proteomics, specifically whether chaperones and other stress-related genes are up- or downregulated in these mutant plants. Although subunit *d* is downregulated in the *shot1-2* mutant (Ch. 1, S. 2), its knockdown alone cannot explain the thermotolerance phenotype of this mutant, especially since knockdown mutants are heat-sensitive (Figure 3.4). Such proteomics data could therefore help to establish further connections between ATP synthase function and the abiotic stress response, as well as inform its specific role – or lack thereof – in the *shot1-2* mutant in particular.

The important need for additional quantitative measurements should also be underscored. While qualitative photographs of RNAi knockdown mutants and pollen are illustrative, they are more effective when accompanied by controlled experiments collecting numerical measurements, such as the width of the *Arabidopsis* rosette or the ratio of viable to nonviable pollen grains. Knowledge of the extent of *ATPQ* knockdown in each line could be confirmed via RT-qPCR and the mutant plants' responses to other forms of abiotic stress can also be helpful for establishing a more concrete relationship between *ATPQ* and the observed phenotypes. Such confirmations can and should be pursued in the future as a supplement to the data presented here.

The work presented here lays an important foundation for further investigations into both the role of the *d* subunit specifically, as well as the importance of ATP synthase and the mitochondrial energetic superstructure, in plant heat stress tolerance. Rising global temperatures and threats to agricultural productivity present a dire prediction for the future. Such potentialities, though, might be avoided as knowledge of plant biology and stress tolerance continues to grow. Even now, there exist strategies for improving thermotolerance in plants using genetic modification technologies (Grover et al. 2013). Such proposals, of course, must be rigorously justified in the scientific, political, and popular forums before they can be

implemented with any real efficacy. In the meantime – optimistically – such incremental advances in plant biology will continue to uncover clues that may someday lead to a more sustainable, efficient, and prosperous global future.

Bibliography

Acebron S.P., Martin I., del Castillo U., Moro F., and Muga A. (2009). DnaK-mediated association of ClpB to protein aggregates. A bichaperone network at the aggregate surface. *FEBS Lett. 583*, 2991-2996.

Baürle, I. (2016). Plant heat adaptation: priming in response to heat stress, *F1000*. *5*, 694.

Bernfur K., Rutsdottir G., and Emanuelsson C. (2017) The chloroplast-localized small heat shock protein Hsp21 associates with the thylakoid membranes in heat-stressed plants. *Prot. Sci. 26*, 1773-1784.

Boyer JS. (1982) Plant productivity and environment, *Science 218*, 443–448.

Breiman A. (2014). Plant Hsp90 and its co-chaperones. *Curr. Protein Pept. Sci*, *15*, 232-244.

Buchanan B.B., Gruissem W., and Jones R.L. (2015) *Biochemistry & Molecular Biology of Plants, Second Edition*, Wiley Blackwell.

Capaldi R.A., Schulenberg B., Murray J., and Aggeler R. (1999) Cross-linking and electron microscopy studies of the structure and functioning of the *Escherichia coli* atp synthase, *J. Exp. Biol. 203*, 29-33.

Che P., Bussell J., Zhou W., Estavillo G., Pogson B, and Smith S. (2010). Signaling from the endoplasmic reticulum activates brassinosteroid signaling and promotes acclimation to stress in *Arabidopsis*, *Sci. Signal*. *3*, 1-12.

Clough S.J. and Bent A.F. (1998) Floral dip: a simplified method for *Agrobacterium*-mediated transformation of *Arabidopsis thaliana, Plant J. 16*, 735-743.

Endo M., Tsuchiya T., Hamada K., Kawamura S., Yano K., Ohshima M., Higashitani A., Watanabe M., and Kawagishi-Kobayashi M. (2009) High temperatures cause male sterility in rice plants with transcriptional alterations during pollen development. *Plant & Cell Phys. 50*, 1911-1922.

Fujikawa M., Sugawara K., Tanabe T., Yoshida M. (2015) Assembly of human mitochondrial ATP synthase through two separate intermediates, F1-c-ring and b-e-g- complex, *FEBS Lett 589*, 2707-2712.

Gajewski E., Steckler D., and Goldberg R. (1986) Thermodynamics of the hydrolysis of adenosine 5'-triphosphate to adenosine 5'-diphosphate, *J. Biol. Chem. 261*, 12733-12737.

Geisler D.A., Päpke C., Obata T., Nunes-Nesi A., Matthew A., Schneitz K., Maximova E.,

Araújo W.L., Fernie A.R., and Persson S. (2012) Downregulation of the δ-subunit reduces mitochondrial ATP synthase levels, alters respiration and restricts growth and gametophyte development in *Arabidopsis*, *Plant Cell 24*, 2792-2811.

Gómez J.F., Talle B., and Wilson Z.A. (2015) Anther and pollen development: A conserved developmental pathway, *J. Integr. Plant Biol 57*, 876-891.

Grover A., Mittal D., Negi M., and Lavania D. (2013) Generating high temperature tolerance transgenic plants: Achievements and challenges, *Plant Sci 205-206*, 38-47.

Hamilton E.W. and Heckathorn S.A. (2001) Mitochondrial adaptations to NaCl. Complex I is protected by anti-oxidants and small heat shock proteins, whereas complex II is protected by proline and betaine. *Plant phys. 126*, 1266-1274.

Hanson M.R., Bentolila S. (2004) Interactions of mitochondrial and nuclear genes that affect male gametophyte development, *Plant Cell 16*, S154-S169.

Hawkins E., Osborne T.M., Ho C.K., and Challinor A.J. (2013) Calibration and bias correction of climate projections for crop modelling: An idealized case study over Europe, *Agric. For. Meterol. 170*, 19-31.

Hong, S. and Vierling, E. (2001). Hsp101 is necessary for heat tolerance but dispensable for development and germination in the absence of stress, *Plant J. 27*, 25-35.

Horst N.A. and Reski R. (2016) Alternation of generations – unravelling the underlying molecular mechanism of a 165-year-old botanical observation, *Plant Biol. 18,* 549-551.

Irish, V. (2009) The flowering of *Arabidopsis* flower development, *Plant Journal 61*, 1014-1028.

Ji. J., Huang W., Yin C., and Gong Z. (2013) Mitochondrial cytochrome c oxidase and F1FO-ATPase dysfunction in peppers (*Capsicum annum* L.) with cytoplasmic male sterility and its association with *orf507* and *ψatp6-2* genes, *Int J Mol Sci 14*, 1050-1068.

Jian Y., Yang B., Harris N.S., and Deyholos M.K. (2007) Comparative proteomic analysis of NaCl stress-responsive proteins in *Arabidopsis* roots, *J Exp Bot 58¸* 3591-3607.

Junge W. and Nelson N. (2015) ATP Synthase, *Annu. Rev. Biochem., 84*, 631-657.

Kim M., Lee U., Small I., des Franc-Small C.C., and Vierling E. (2012) Mutations in an *Arabidopsis* mitochondrial transcription termination factor-related protein enhance thermotolerance in the absence of the major molecular chaperone HSP101, *Plant Cell. 24¸*3349-65.

Lavania D., Dhingra A., Siddiqui M.H., Al-Whaibi M.H., and Grover A. (2015). Current status of the production of high temperature tolerant transgenic crops for cultivation in warmer climates, *Plant Phys & Biochem. N.v.*, 1-9.

Lee U., Wie C., Escobar M., Williams B., Hong S., and Vierling E. (2005). Genetic analysis reveals domain interactions of *Arabidopsis* HSP100/ClpB and cooperation with the small heat shock protein chaperone system. *Plant Cell. 17*, 559-571.

Li W.Q., Zhang X.Q., Xia C., Deng Y., and Ye D. (2010) MALE GAMETOPHYTE DEFECTIVE 1, encoding the Fad subunit of mitochondrial F1FO-ATP Synthase, is essential for pollen formation in *Arabidopsis thaliana*, *Plant Cell Physiol 52*, 923-935.

Lobell, D., Schlenker, W., and Costa-Roberts, J. (2011). Climate trends and global crop production since 1980, *Science. 333*, 616-620.

McLoughlin F., Basha E., Fowler M., Kim M., Bordowitz J., Katiyar-Agarwal S., and Vierling E. (2016). Class I and II small heat shock proteins together with HSP101protect protein translation factors during heat stress. *Plant Physiol. 172*, 1221-1236.

Meinke D.W., Cherry J.M., Dean C., Rounsley S.D., and Koornneef M. (1998) *Arabidopsis thaliana:* a model plant for genome analysis. *Science 282*, 662-682.

Melillo J.M., Richmond T.C., and Yohe G.W. (2014) Climate Change Impacts in the United States: The Third National Climate Assessment. *U.S. Global Change Research Program*.

Mittler, R., Finka, A., and Goloubinoff, P. (2012). How do plants feel the heat? *Trends Biochem. Sci. 37*, 118-125.

Mogk A., Kummer E., and Bakau B. (2015). Cooperation of Hsp70 and Hsp100 chaperone machines in protein disaggregation, *Front. Mol. Biosci. 2*, 22.

Müller F. and Rieu I. (2016) Acclimation to high temperature during pollen development, *Plant Reprod. 29*, 107-118.

Neuwald A.F., Aravind L., Spouge J.L., and Koonin E.V. (1999). AAA+: A class of chaperone-like ATPases associated with the assembly, operation, and disassembly of protein complexes. *Genome Res. 9*, 27-43.

Ogawa M., Kay P, Wilson S., Swain S.M. (2009) ARABIDOPSIS DEHISCENCE ZONE POLYGALACTURONASE1 (ADPG1), ADPG2, and QUARTET2 are polygalacturonases required for cell separation during reproductive development in *Arabidopsis*. *P. Cell 21*, 216-233.

Park C. and Seo Y. (2015). Heat shock proteins: a review of the molecular chaperones for plant immunity. *Plant Pathol. J. 31,* 323-333.

Pucciariello C., Banti V., Perata P. (2012) ROS signaling as common element in low oxygen and heat stress. *Plant Phys & Biochem 59,* 3-10.

Qu A., Ding Y., Jiang Q., and Zhu C. (2013). Molecular mechanisms of the plant heat stress response, *Biochem. & Biophys. Res. Comm. 432,* 203-207.

Rees D., Leslie A.G.W., and Walker J.E. (2009) The structure of the membrane extrinsic region of bovine ATP synthase. *Proc Nat Acad Sci 106,* 21597-21601.

Rosenzweig R., Moradi S., Zarrine-Afsar A., Glover J.R., and Kay L.E. (2013). Unraveling the mechanism of protein disaggregation through a ClpB-DnaK interaction. *Science. 339,* 1080-1083.

Saidi Y., Finka A., Muriset M., Bromberg Z., Weiss Y., Maathuis F., and Goloubinoff P. (2009). The heat shock response in moss plants is regulated by specific calcium-permeable channels in the plasma membrane, *Plant Cell. 21,* 2829-2843.

Sanchez Y., Lindquist S.L. (1990). HSP104-required for induced thermotolerance. *Science. 248,* 1112-1115.

Scheler C., Durner J., and Astier J. (2013) Nitric oxide and reactive oxygen species in plant biotic interactions, *Curr Opin Plant Bioli 16,* 534-539.

Schroda, M., Hemme, D., and Mühlhaus, T. (2015). The *Chlamydomonas* heat stress response, *Plant J. 82,* 466-480.

Scott R., Spielman M., and Dickinson H. (2004) Cytochemistry of pollen development in *Brachypodium distachyon*. Plant Syst Evol *300,* 1630-1648.

Scutt C.P. and Vandenbussche M. (2014) Current trends and future directions in flower development research, *Ann. Bot. 114,* 1399-1406.

Selinski J. and Scheibe R. (2014) Pollen tube growth: where does the energy come from? *Plant Sig. Behav. 9,* e977200.

Sika K.C., Kefela T., Adouknou-Sagbadja H., Ahoton L., Saidou S., Baba-Moussa L., Jno Baptist L., Kotconi S.O., Gachomo E.W. (2015) A simple and efficient genomic DNA extraction protocol for large scale genetic analyses of plant biological systems. *Plant Gene 1,* 43-45.

Sobti M., Smits C., Wong A.S., Ishmukhametov R., Stock D., Sandin S., and Steward A.G. (2016) Cryo-EM structures of the autoinhibited *E. coli* ATP synthase in three rotational states. *Elife 5*: n.p.

Sun X., Wheeler C.T., Yolitz J., Laslo M., Alberico T., Sun Y., Song Q., and Zou S. (2014) A mitochondrial ATP synthase subunit interacts with TOR signaling to modulate protein homeostasis and lifespan in *Drosophila*, *Cell Rep 8*, 1781-1792.

United Nations, Department of Economic and Social Affairs, Population Division (2017) *World Population Prospects: The 2017 Revision, Key Findings and Advance Tables*.

Valin H., Sands R.D., van der Mensbruggh D., Nelson G.C., Ahammad H., Blanc E., Bodirsky B., Fujimori S., Hasegawa T., Havlik P., Heyhoe E., Kyle P, Mason-D'Croz D., Paltsev S., Rolinski S., Tabeau A., van Meijl H., von Lampe M., and Willenbrockel D. (2014). The future of food demand: understanding differences in global economic models, *Agric. Econ. 45*, 51-67.

van Norman J.M. and Benfey P.N. (2009). *Arabidopsis thaliana* as a model organism in systems biology. *Wiley Interdiscp Rev Syst Biol Med. 1*, 372-379.

Welch A., Bostwick C.J., and Cain B.D. (2010a) Manipulations in the peripheral stalk of the *Saccharomyces cerevisiae* F1FO-ATP Synthase, *J. Biol. Chem. 286*, 10155-10162.

Welch J.R., Vincent J.R., Auffhammer M., Moya P.F., Dobermann A., and Dawe D. (2010b) Rice yields in tropical/subtropical Asia exhibit large but opposing sensitivities to minimum and maximum temperatures, *Proc. Nat. Acad. Sci. 107*, 14562-14567.

Wittig I. and Schägger H. (2008) Structural organization of mitochondrial ATP synthase. *Biochim. Biophys Acta 1777*, 592-598.

Appendix: Supplemental Information

Primer Sequences (5' to 3')

ATPQ and *atpq-1* PCR

ATPQ *Gene Primers*

- ATPQ-F2: GCCCACTACATTTCCAATTCC
- ATPQ-R2: GAGAGTTTTCTTTCCAAGCCG

T-DNA Primer for atpq-1:

- SAIL-LB3: TAGCATCTGAATTTCATAACCAATCTCGATACAC

Quartet Mutant PCR

QRT2 *Gene Primers*

- QRT2-LP: TATCGATAGTGAGTGGGTCGG
- QRT2-RP: TGGGGATCAAAAGTGATCAAG

T-DNA Primer

- LBb1.3: ATTTTGCCGATTTCGGAAC

RNAi Knockdown Primers

- ATPQ-F4: CACCAAAGCTCAGCACCATGACTG
- ATPQ-R4: TCACTGAAGAACGAAACGAAACA
- ATPQ-F5: GACTCTAGAGGCGCGCCAAAGCTCAGCACCATGACTG
- ATPQ-R5: GACGGATCCATTTAAATTCACTGAAGAACGAAACGAAACA

Clustal Omega Comparison Sequence Accession Numbers

Arabidopsis lyrata: ARALYDRAFT_485596
Glycine max: GLYMA10G35750
Hordeum vulgare: MLOC_21708
Oryza sativa: OJ1666_A04.19
Zea mays: ZEAMMB73_Zm00001d031825

ATP Synthase Subunits Across Model Organisms

E. coli ATP Synthase	Chloroplast ATP Synthase	Animal Mitochondrial ATP Synthase	Plant Mitochondrial ATP Synthase
α	α	α	α
β	β	β	β
γ	γ	γ	γ
δ	δ	OSCP	O/OSCP or δ’
ε	ε	δ	δ
-	-	ε	ε
a	a (subunit IV)	a (subunit 6)	a (subunit 6)
b (or b, b’)	b and b’ (subunits I, II)	b and b’ (subunit 4)	*orf25* (b or 4 homolog)
c	c (subunit III)	c (subunit 9)	c (subunit 9)
-	-	d	d
-	-	e	?
-	-	f	?
-	-	g	?
-	-	h	?
-	-	A6L or 8	8 (*orfB*)
-	-	F_6	?
-	-	IP or IF or IF1 (inhibitor)	IP or IF or IF1 (inhibitor)
-	-	F_B or Factor B	?
-	-	-	F_Ad (plant-specific)

Known Genes Encoding Plant Mitochondrial ATP Synthase Subunits

Courtesy of www.uniprot.com

α: **mitochondrial**, Atmg01190

β: **nuclear**, At5g08690

γ: **nuclear**, At2g33040

δ: **nuclear**, At5g47030

ε: **nuclear**, At1g51650

a: **mitochondrial**, Atmg00410, Atmg01170 (two identical copies)

b: **mitochondrial**, Atmg00640 (possible b subunit, *orf25*) (Heazlewood et al. 2013, *FEBS Lett 540*: 201-205).

c: **mitochondrial**, Atmg01080

d: **nuclear**, At3g52300

OSCP: **nuclear**, At5g13450

A6L/8: **mitochondrial,** Atmg00480

F_Ad: **nuclear**, At2g21870